Paula Martínez Cánovas

POROSITY DETERMINATIONS OF ELECTROSPUN NANOFIBERS BY MICROSCOPY TECHNIQUES

MASTER'S DEGREE THESIS

supervised by Dr. Joan Rosell-Llompart and Ph.D. student Reyda Akdemir

MASTER'S DEGREE IN NANOSCIENCE, MATERIALS AND PROCESSES

UNIVERSITAT
ROVIRA i VIRGILI

Tarragona

2020

Porosity determinations of electrospun nanofibers by microscopy techniques

Porosity determinations of electrospun nanofibers by microscopy techniques

Paula Martínez Cánovas[1], Reyda Akdemir[1] and Joan Rosell-Llompart[1,2]

[1]*Department of Chemical Engineering, Universitat Rovira i Virgili, Avda dels Països Catalans, 26, 43007 Tarragona, Spain*
[2] ICREA *(Catalan Institution for Research and Advanced Studies), Barcelona, Spain*

E-mail: paula.martinezca@estudiants.urv.cat

Abstract

Porous micro- and nanofibers can be produced easily by electrospinning technique. In this research proposal, we review the literature on porous electrospun nanofibers, the mechanisms to create internal porous electrospun fibers and its applications in different fields, ranging from oil sorption to sensors, lithium-ion batteries, photocatalysis and drug delivery. The previous characterization methodologies (such as physical nitrogen adsorption method (BET), mercury intrusion and thermoporometry) are analyzed alongside with their drawbacks. Our proposal aims to overcome the limitations of the previous characterization methodologies in order to determine the porosity of electrospun nanofibers (intra-fiber porosity) with the combination of Scanning Electron Microscopy (SEM) and Atomic Force Microscopy (AFM).

Keywords: electrospinning, intra-fiber porosity, nanofiber

1. Background ad state of the art

1.1. General Introduction

Electrospinning is a versatile and flexible technique that allows the generation of ultrathin micro- and nanofibers. This method makes use of a high-voltage to produce an electrical field in order to elongate and stretch a polymer solution into a jet to a conductive collector. The polymer solution displays a viscoelastic behavior and is stretched until the bending instability of the jet, where the plastic deformation occurs with a growing loop, also termed as "whipping motion". The fibers are produced when the solution is solidified and placed onto a deposition surface (collector).[1–4]

Fibers can be produced with different morphology,[5] since beaded fibers,[6] hollow fibers,[7] porous fibers,[8] or uniform fibers[9] to helical fibers.[10] Besides, the alignment of the fiber can be controlled, providing a random[11] or aligned[9] distribution of them onto the collector.

Depending on the type of collectors one can get different types of nanofibers. With this aim, collectors can be classified into two main categories. The former is the stationary collectors, which are motionless and the nanofibers are deposited randomly. Likewise, the latter is the dynamic collectors, which use the movement of the collector for achieving aligned fibers or a thickness diameter of the nanofiber. Among the stationary collectors, plate and ring collectors placed in parallel[12] are examples of the possible configurations. Within the dynamic collectors, there are many shapes,[13] such as rotating cylinder,[9] wire drum,[14] disc,[15] and tube collectors.[16]

For the purpose of achieving aligned electrospun nanofibers, the whipping motion can be eliminated by collecting them on a rotating cylinder by means of a back electrode near to the tip of the needle and a collector

surface rate equal or higher than the speed of the Fiber Production Rate, FPR, as Kiselev and Rosell-Llompart reported in their study. This FPR can be defined as the rate at which nanofibers are fabricated and can be modified by using the syringe pump. Furthermore, the back electrode creates a uniform electric field between the needle and the rotating collector due to its squared geometry.[9] Therefore, mechanical and electrostatic forces are involved in the abovementioned work, but also the magnetic force can be taken into account for the alignment of fibers through two parallel-positioned permanent magnets and a small number of magnetic nanoparticles (less than 0.5 wt%) in the polymer solution.[17] Otherwise, a magnetic force can be used without the magnetic nanoparticles through two bar magnets with a field in the opposite direction that the ejected polymer solution.[18]

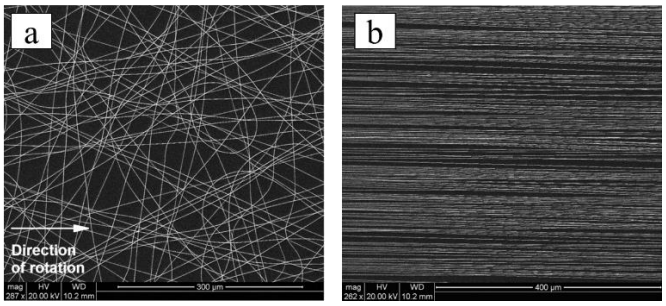

Figure 1. SEM images of polystyrene (PS) electrospun fibers: (a) random distribution of the fiber, (b) aligned distribution of fibers. Adapted with permission.[9] Copyright 2012 Wiley Periodicals, Inc.

Another way to control the morphology of electrospun nanofibers is the type of nozzle. The most common nozzle used to generate nanofibers by electrospinning is a hollow needle. Other nozzle types have been used, however. In general, the spinneret can be solid (e.g. a solid pin, a 2D array of solid pins or a flat substrate) or hollow (e.g. a hollow needle or a tube with holes inside). Therefore, the solid spinneret provides an unconfined feed that flows unrestricted over the surface of another material. It can use a flat plate to produce multiple jets from a single orifice at the same time.[19] Regarding the hollow spinneret, it supplies a confined system and the polymer solution is extruded along a needle with a typical range of 0.3-1.0 mm or a tube with multiple holes or apertures in the wall, creating an array of jets.[1]

Applications of produced nanofibers via electrospinning are included in a wide range of fields, such as catalysis,[20] scaffold and tissue engineering,[21] solar cells,[22] membranes of filtration,[23] among others. Solution blow spinning is another method to produce polymeric nanofibers in which a polymeric solution is injected through an accelerated gas stream (e.g. nitrogen, argon, or air) without a high power supply. In contrast, the gas flow pressure and the processing parameters (concentration, type and injection rate of polymer solution) highly affect to the fabricated fibers because the driving forces of solution blow spinning are mainly physical ones, instead of electrical forces as for electrospinning.[24]

Nowadays, porous electrospun nanofibers have gained importance due to their pivotal role in some applications that this work reviewed. Thereby, the porosity in electrospinning has been studied as the inter-fiber porosity or "mat porosity", with no special attention paid to the intra-fiber porosity or "fiber porosity".

Our proposal aims to develop a new characterization methodology for the determination of the intra-fiber porosity of electrospun nanofibers. This proposal provides a solution for the limitation of the previous methods for characterizing the interior porosity due to the smooth surface in fibers, involving an important hindrance to access at the interior pores.

1.2. Importance of fiber porosity

1.2.1. Definitions

Recent research on porous electrospun nanofibers[1,25,26] has explored the intra-fiber porosity that has received much less attention than the inter-fiber porosity or "mat porosity". While inter-fiber porosity is defined as the voids between electrospun fibers inside a membrane, intra-fiber porosity can be classified into two types: surface and internal porosity. The surface porosity includes all the pores in the shell along the length of the fibers[27,28] and internal porosity involves the porous inside the fibers that can be also called "interior porosity" or "in-fiber porosity".[1,26]

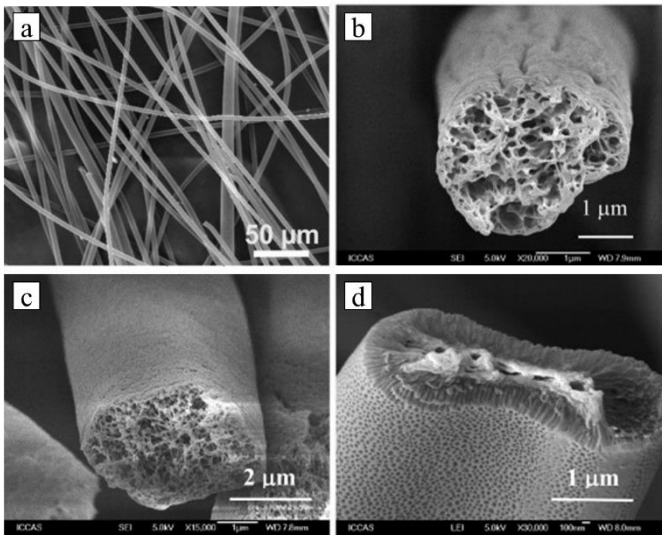

Figure 2. SEM images of polystyrene (PS) electrospun nanofibers. (a) Inter-fiber porosity of a mat. Cross-section images that show intra-fiber porosity: (b) internal porosity, (c) internal porosity, (d) surface porosity. (a) Adapted with permission.[11] Copyright 2012 Elsevier (b, c, and d) Adapted with permission.[29] Copyright 2012 Elsevier.

1.2.2. Role of fiber porosity in applications

One unique property of electrospun fibers is their high inter-fiber porosity which provides an increase of the specific surface area alongside a higher photocatalytic activity.[30] Besides, the catalysis field is another profitable field as a consequence of the high activity and stability of porous nanofibers compared to the compact fibers.[31]

One of the greatest challenges in recent studies is to determine how to control the internal fiber porosity, due to it plays a critical role in many technological applications, such as oil sorption, bone scaffolds, photocatalytic activity, drug delivery, lithium-ion batteries, and mechanical strength.

An example of oil sorption was carried out by Bandegi and Moghbeli, who analyzed the role of solvent quality and humidity on the porous formation in individual styrene/acrylonitrile copolymer (SAN) electrospun nanofibers. These SAN nanofibers showed a higher oil absorbency compared to the non-porous nanofibers.[32]

The combination of internal and surface porosity is also an advantage in the oil adsorption field, as Isık and Demir mentioned in their study about tailored electrospun fibers from waste polystyrene for high oil absorption. Therefore, they tested the oil absorption with five different foam-expanded polystyrene (f-PS) concentrations. The results showed that the fibers with interior porosity and surface texture have a high adsorption capacity.[33]

A further study of interest was performed by Zaarour *et al.*, where they generated several polyvinylidene fluoride (PVDF) nanofibers with secondary surface morphology (porous surfaces, rough surfaces, grooved surfaces, and internal porosity) with different relative humidity values and solvent mixtures ratios of acetone and N,N-Dimethylformamide. Therefore, macro-porous PVDF nanofibers with interior pores evidenced the higher specific surface area and pore volume. As a result, the highest oil absorption capacity was directly connected with this aforementioned secondary structure.[8]

The ultrahigh oil (silicone oil, pump oil, sunflower oil, and diesel) adsorption capability was also studied by Chen and Tung, who fabricated different PS electrospun fibers morphology via one-step electrospinning at several solvent/nonsolvent mixtures ratios (chlorobenzene (CB) and dimethyl sulfoxide (DMSO), respectively). Moreover, they reported that open microscale holes inside fiber structures demonstrated rapid adsorption alongside a high adsorption capability.[34]

Thereby, Mota *et al.* reported a published study in the tissue engineering field with the aim to develop poly [(R)-3-hydroxybutyrate-co-(R)-3-hydroxyhexanoate] (PHBHHx) electrospun microstructures with a layer-by-layer control for the well-defined internal architecture and external shape of the scaffolds. Referred to the highly porous morphology of the nanofibers, several advantages are found, such as the biodegradation rate, the mass transfer associated with cell metabolism and the mechanisms regulating cell adhesion and proliferation. All of them are crucial for enhanced development of the bone scaffolds inside the human body.[35,36]

It is noteworthy the reported work by Hou and co-workers about the production of hierarchically porous TiO_2/SiO_2 fibers to enhance the photocatalytic activity, avoiding the separation problems (from the reaction solution after the photocatalytic procedure) connected with TiO_2 nanoparticles without support. Therefore, the abovementioned fibers were capable to keep all the advantages own of nanoparticles (high efficiency, low cost, chemical inertness, and high specific area), but also to photodegrade rhodamine B (RhB) with higher efficiency, high thermal stability and uniformity.[37]

Another advantageous technology is the biodegradable drug delivery owing to the enhancement of diffusion and the structure's fluid transport due to a highly porous morphology of electrospun nanofibers. It is a consequence of decreasing the density of nanofibers in comparison with produced fibers by melted-based techniques (e.g. melt electrospinning).[38,39]

In the lithium-ion batteries field, Sabetzadeh *et al.* reported the pivotal role of the highly porous PAN nanofibers as separators in order to facilitate and enhance the ion migration due to its higher discharge capacity.[40] Otherwise, a separator membrane with ultrafine fiber for the abovementioned field can be fabricated through other techniques, such as melt-blown spinning, melt-electrospinning or sea-island melt spinning.[41]

Regarding the textile approach, Yan *et al.* reported a multi-scaled interconnected inter- and intra-fiber porous Janus membranes for enhanced directional moisture transport in a dual-layer for sportswear in order to transfer the humidity from skin to the atmosphere and avoiding reverse transport. With this aim, the electrospun superhydrophilic hydrolyzed porous polyacrylonitrile (HPPAN) nanofibers for one of the parts of the membrane and hydrophobic polyurethane (PU) fibers lead to the fact that water can access through the positive direction (PU fibers on the top), but it cannot in the reverse direction (HPPAN nanofiber layer on the top). In this sense, the porous structure of HPPAN fibers increases the wicking rate through more pathways alongside a positive Laplace pressure for the enhancement of fast transport of water.[42]

Kim and co-workers reported a study for creating nanoporous polymethylmethacrylate (PMMA) electrospun fibers, making use of cellulose nanocrystals (CNCs) in the electrospun solution. The utilization of hygroscopic CNCs raises the water condensation in the nonsolvent induced phase separation at high relative humidity, which produces a higher intra-fiber porosity in the electrospinning technique. Thus, the sensitivity and response time of a gas sensor (a microfabricated quartz tuning fork, QTF) is enhanced compared to the non-nanoporous structures.[43]

Biosensing is a field that also benefits from the intra-fiber porosity of electrospun nanofibers. Thereby, Nathani and Sharma published an article about the increase of sensitivity of porous poly(styrene-block-methyl-methacrylate) (PS-b-PMMA) nanofibers liken to the as-spun nanofibers for electrochemical biosensors.[44]

1.3. Methodologies to create internal porous electrospun fibers

There are several methods with the objective of creating internal porous electrospun fibers. Thus, they can be divided into mechanisms without a heat-treatment process after the electrospinning technique or with a heat-treatment process. Likewise, several parameters are involved in the mechanism to generate intra-fiber porosity, such as the temperature, miscibility, conductivity, and crystallinity. In this sense, it is possible to distinguish the following mechanisms:

1.3.1. Porosity induced by Selective Removal of a Sacrificial Phase

According to the sacrificial phase, small molecules, block copolymers, polymers or nanoparticles can be involved. In this sense, calcination and leaching processes are crucial for the removal step that allow the degradation of the aforementioned particles, which are inside the polymer to generate pores instead.[1,45–48]

Furthermore, the porous carbon and carbon-based fibers are some of the most relevant types of fibers where the heat treatment is critical for the intra-fiber porosity. Therefore, CFs can be produced by spinning a polymer precursor solution with high carbon content and high molecular weight. Following that, the pyrolysis process is placed, where the polymer precursor is converted into CFs. This procedure can be called oxidation stabilization (oxygen-containing atmosphere in a range of temperature from 180ºC to 300ºC), carbonization (inert conditions) and graphitization (until 300ºC) or activation (oxidizing atmospheres with a range of temperature of 700-1200ºC) depending on its temperature and atmosphere conditions, in the case of polyacrylonitrile (PAN)-based fibers.[49]

For the purpose to create porosity, it is indispensable to induce phase separation with a guest precursor that is added in the polymer precursor solution, also called the home precursor. In this way, the guest precursor is utilized as a sacrificial phase for selective removal during thermal treatment.[25] Guo *et al.* provided the preparation of Fe/Ni,N-doped porous carbon fibers (Fe/Ni-NPCF). After the electrospun step, fibers were placed into a melamine boat and the heat treatment was carried out, starting at 280ºC with a heat rate of 2ºC/min for 2 h in air. Subsequently, the annealing process occurred at 800ºC for 1h with a ramping rate of 5ºC/min

in a nitrogen atmosphere and a following SiO_2 removal with a KOH solution.[50]

TiO_2 fibers are another important example of porous fibers that are produced by a selective removal of the sacrificial phase. In this case, the heat treatment is a calcination process at high temperature (500ºC) for the transformation of metal alkoxides (precursor) such as titanium tetraisopropoxide $[Ti(O_iPr)_4]$[51] into pure TiO_2 or TiO_2/C fibers with random porosity.[25] With the aim to achieve a homogeneous pore size, hollow structure, and controlled morphology, particulate templates are added such as $CaCO_3$[52] or polystyrene nanospheres.[53] In this way, templates act like molding for the final internal porosity. In addition, some ionic liquids can be included with the sol-gel method to create a mesoporous structure like Lin *et al.*, who reported the pivotal role of the 1-butyl-3-methylimidazolium tetrafluoroborate ($[BMIM^+][BF^{4-}]$) for 1-D mesoporous formation.[54]

1.3.2. NSIPS (non-solvent induced phase separation): TIPS (thermally induced phase separation) and VIPS (Vapor Induced Phase Separation)

The aim of this procedure is the separation of a homogeneous polymer solution in two liquid phases (polymer-rich and polymer-poor). For this purpose, two processes exist. [57]

One of them is the thermally induced phase separation (TIPS), where the temperature should be decreased below the upper critical temperature (UCST).

The second one is the non-solvent induced phase separation (NSIPS), in which the non-solvent (such as water) should be added into the polymer solution. In this proceeding, Thermodynamics plays an important role since there is an unstable region, called the demixing gap, where separation in two phases occurs.

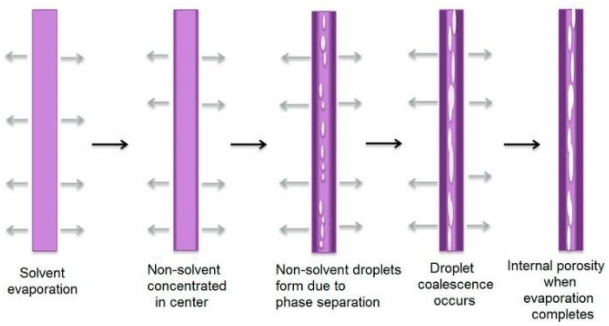

Figure 3. Schematic figure of the created pores by non-solvent induced phase separation (NIPS). Adapted with permission. [58] Copyright 2018 Elsevier.

Furthermore, vapor induced phase separation (VIPS) is involved as a particular type of non-solvent induced phase separation (NSIPS) or thermally induced phase separation (TIPS). In this mechanism, the water, which is a non-solvent vapor, is introduced (dissolved) and mixed inside the fiber. Subsequently, the solvent is evaporated and the phase separation supplies the liquid-liquid demixing due to the concentration of the polymer is thermodynamically unstable and the boiling point of the solvent is higher in comparison with water (slow evaporation of solvent). In this sense, the phase separation carries on the coexistence of polymer-rich and polymer-poor phases.[59]

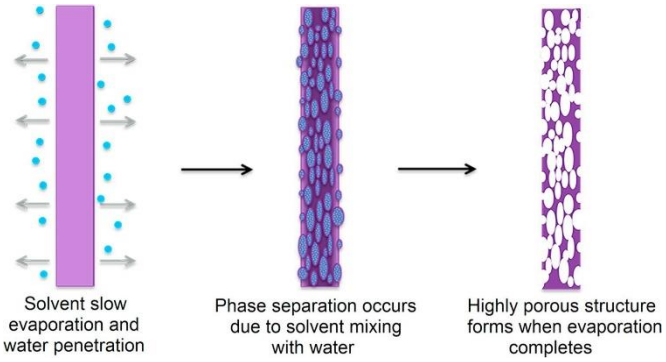

Figure 4. Schematic figure of created pores by vapor induced phase separation (VIPS) mechanism. Adapted with permission. [58] Copyright 2018 Elsevier.

The main characteristic of this process is a porous internal structure and a smooth surface.[9] For this system, solvent vapor pressure should be below and also, solvent and water should be miscible.

1.3.3. Construction of internal porosity (secondary structures) using solvent mixtures (solvent/non-solvent mixtures, solubility, conductivity, and NSIPS).

Several researchers have developed numerous studies connected with this topic, and the work performed by Jeun *et al.* is an example of these. Therefore, they analyzed the utilization of different solvent/non-solvent mixtures for PCL nanofibers such as chloroform solvent with DMF, hexane, and methanol as non-solvents where are involved different solubility parameters and dipole moments of each solvent.[5] In another work, Semiromi *et al.* reported the increase of the conductivity for the electrospinning process due to the PCL has an excellent solubility with chloroform, but this PCL/chloroform system is not favorable for the electrospun mechanism.

In this sense, the use of methanol provides a reduction of the fiber diameter that also affects the internal porosity due to the evaporation is faster and consequently, the porosity is minor yielded by the processing time is not enough for the porous formation.[60] Otherwise, the non-solvent induced phase separation (NSIPS) is also relevant in the last type of mixtures and thus, the lower volatility of methanol compared to chloroform that enhances the last-mentioned mechanism.

1.3.4. Porosity created after a vitreous skin forms early in the evaporation process. Vitrification process (physical gelation).

Vitrification mechanism or physical gelation is related to the solution of semicrystalline or crystalline polymers, where the polymer crystals perform as a physical junction point to supply the form of a 3-D network. It involves the process where evaporation occurs quickly and the solubility of the polymer within the solvent is low. In this way, the concentration of the solute building upon the surface of the fiber exceeds the solubility limit, the diffusion rate of non-solvent is reduced by the gelled surface and the solute precipitates out forming a glassy skin, which does not collapse forcing the appearance of voids after the left of the remaining solvent, or collapses partially, also leaving voids inside (commonly "large").[61]

1.3.5. Coaxial electrospinning.

Co-electrospinning technique is a procedure where a spinneret with two coaxial capillaries (coannular nozzles) or a single-nozzle (annular nozzle), with two polymeric solutions, generates core/shell electrospun micro- and nanofibers. Likewise, the hollow fibers are produced due to the core of the nanofiber being removed by an evaporation process, utilization of solvents or heat treatment (calcination or pyrolysis). The evaporation without the distortion of the shell is possible because the solidification of the shell is faster.[62] Furthermore, the coannular nozzles have some drawbacks in comparison with the single-nozzles, such as the difficulty of achieving a good concentricity of the core/shell.[7]

Regarding the polymer solutions, they should be sufficiently viscous to elongate in a jet without discontinuities. In addition, they should have a similar dielectric property to provide a similar electrical force in the ejection process. However, the inner fluid can be an insulating material if the outer fluid supports it with enough pressure.[63] Another crucial condition is the immiscibility of the polymer-solvent to achieve a stabilized co-electrospinning process with a solid film in the interface that separates both phases. Additionally, the core/shell diameter of the hollow fibers is directly connected with the shell-to-core solution flow-rate ratio and for this reason, it is a pivotal parameter to control in the co-electrospinning mechanism.[1,62]

It is noteworthy the approach of creating multi-channel tubular structures, such as the three-channel tube (TCT) fabrication system. In this way, three metallic capillaries or more in a plastic syringe allow the generation of multi-hollow fibers with higher specific surface area.[63]

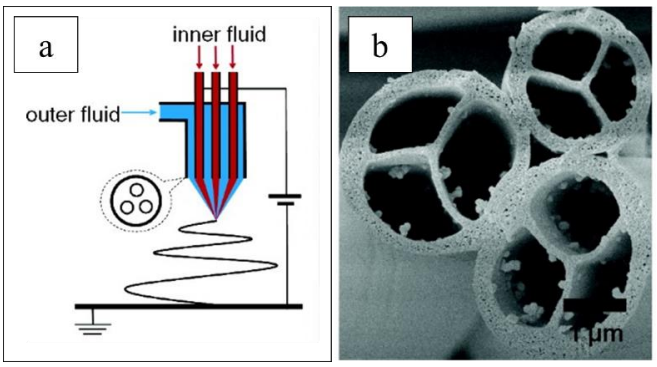

Figure 5. (a) Schematic figure of the three-channel tube system. (b) Cross-section images of hollow fibers. Adapted with permission.[63] Copyright 2007 American Chemical Society.

1.3.6. Emulsion electrospinning

Zhang *et al*. reported the vital role of emulsion electrospinning that overcomes the limitations for creating a mesoporous and hollow structure (laborious process and unstable flux) of older techniques, such as coaxial electrospinning and multi-fluidic electrospinning. This technique started with the precursor solution of an emulsion system, which is composed of metal alkoxide and the oil phase. Subsequently, the electrospun took place during 10 h with a decomposition into inorganic oxides at 110ºC for 12h to achieve a dense film by the crosslink of the inorganic framework. Finally, the fibers were calcined at 500ºC for 4 h in air with a heating rate of 1ºC/min to pyrolyze the organics. As a result, the porous TiO_2-SiO_2 nanofibers are fabricated.[64]

Otherwise, the microemulsion precursor system typical of the oil is useful for the pore generation. Regarding this, Chen *et al*. analyzed the fabrication of

hierarchically porous inorganic fibers by a microemulsion of paraffin oil before the electrospinning and calcination process.[55]

1.4. Methodologies to characterize intra-fiber porosity of electrospun fibers

Different characterization methodologies have been explored along the time to analyze the intra-fiber porosity of electrospun fibers.[11]

1.4.1. BET (Brunauer, Emmett and Teller)

The BET (Brunauer, Emmett and Teller) surface area, based on a physical nitrogen adsorption technique (at a temperature of 77K), has been used for determining the specific surface area of porous materials, such a porous nanofiber. However, the characterization of the interior porosity is a problem in this technique due to the difficulties in accessing the internal voids with a smooth surface. Consequently, its utilization is limited and the empirical process of BET for the isotherm analysis needs a blank test (non-porous reference materials), with the aim of facilitating the interpretation of data.[65]

1.4.2. Mercury intrusion

Another porosimetry procedure is the mercury intrusion, where mercury, as a non-wetting liquid, penetrates into pores as a consequence of applying the postulated minimum pressure of Washburn. Therefore, the macro- and mesopore size distribution can be measured inside a porous solid, considering that mercury enters pores in decreasing order of size or by their interconnection system. Another assumption of this method is that the obtained radius is an equivalent of the cylindrical radius in a theoretical pore. Thus, the shape of pores is not present in the volumetric distribution, only the mean pore size, pore size distribution, and total pore volume. Hence, an important disadvantage of the mercury intrusion is the possible damage of the samples and the lower resolution with the purpose of analyzing nanopore size distribution of electrospun fibers.[65,66]

1.4.3. Thermoporometry

Thermoporometry or thermoporosimetry is a method directly connected with the temperature depression after a melting or crystallization process is caused by a solid-liquid phase transition. The change of temperature occurs in a probe liquid into a pore (condensed adsorbate) and it is determined with the help of a Differential Scanning Calorimetry (DSC) system. Thereby, the internal pore size can be measured in a range of 1.5 to 150 nm (mesoporous material). For the purpose of manipulating a good adsorbate liquid, water is used as the most common due to its heat of fusion (H_f = 334 J/g) is larger than the majority of organic liquids and it is more sensitive for the temperature shift in little volumes. In order to avoid the possible distortion in measurements of physical parameters (e.g. contact angle, heat of fusion or surface tension), a reference material without porous should be measured like in the abovementioned characterization methodologies.[65,67]

1.4.4. Density measurement

Density measurement of porous electrospun nanofibers is a versatile method to determine the interior porosity of them through the utilization of a nonpolar and hydrophobic liquid paraffin. These two conditions are crucial for avoiding the wetting process with the nanofibers as Fashandi and Karimi reported in their study.[11] Therefore, making use of the total volume of the vessel and knowing the mass of electrospun nanofibers as well as the mass of the matrix, it is possible to calculate the density of the mixture. In this way, the weight fraction of the fibers and matrix is also known and the total pore volume of the electrospun nanofibers can be determined.

1.4.5. Focused Ion Beam and Scanning Electron Microscopy (FIB-SEM) 3D reconstruction

Focused Ion Beam (FIB) and Scanning Electron Microscopy (SEM) can be combined in order to get a 3D reconstruction imaging and a 2D analysis. The 3D tomography image is obtained by the 'slice-and-view' methodology, which uses the FIB sectioning for cutting along the sample several times and the SEM for analyzing the cross-sectional images of the sample. Therefore, the compilation of all the cross-section SEM images provides a complex 3D analysis of a porous structure. Thereby, the software Image J (version 1.46r, NIH, U.S.A.) collects the SEM images and the Resolve RT (Avizo fire, version 5.2 - FEI Edition, Ger.) allows the 3D reconstruction. Accordingly, the pore size and pore shape is determined by this method, and also, the distribution of the pores (or voids) inside the sample with a high spatial resolution. However, we have not found evidence of this approach with pores of single nanofibers, only with electrospun mats, cell structure, or single microfibers.[68] This characterization methodology

provides more information than the conventional one, although more complexity. Even so, this characterization supplies a new optimization of the evaluation of the experimental work that can be developed in the intra-fiber porosity of the electrospinning field.[69,70]

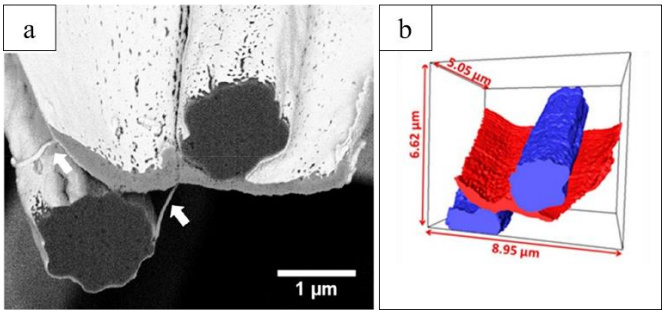

Figure 6. FIB-SEM tomography of the cell attached to PVDF (+) scaffolds: (a) SEM image of a cross-section of cell and microfibers, (b) 3D reconstruction of a cell into two microfibers. Adapted with permission.[71] Copyright 2019 American Chemical Society.

1.4.6. Scanning Electron Microscopy (SEM)

Scanning Electron Microscopy (SEM) is an optical microscopy technique based on the interaction between the secondary electrons and a sample. It is commonly used for taking images of the samples with a magnification up to the nanoscale, such as the cross-section of the electrospun nanofibers[72] or the random distribution of the fibers in a mat.[36] This optical characterization allows qualitative knowledge about the morphology of the samples and quantitative knowledge about the chemical composition. In contrast with the previous characterization methods which have been explained, this method doesn't provide a value of the porosity single-handedly. However, it can be combined with other characterization techniques (such as FIB) for determining the intra-fiber porosity.

1.4.7. Field Emission Scanning Electron Microscopy (FE-SEM)

Field Emission Scanning Electron Microscopy (FE-SEM) is an optical microscopy technique with a higher resolution in the topographic images than the SEM (2-3 nm) and with a lower accelerating voltage (under 5 kV).[73] Therefore, this characterization method supplies a better approach in the optical field in comparison with SEM. Moreover, the higher resolution magnifies the pores that need more contrast to be resolved, but the limitations are similar to the SEM due to the determination of the pore volume is not possible by itself.[58]

1.4.8. Limitations of each one of the existing characterization methodologies

Regarding the limitations of the aforementioned characterization methodologies for the intra-fiber porosity of electrospun fibers, it is noteworthy that the main disadvantage is the determination of the interior pores in fibers with smooth surfaces. Thereupon, the BET surface area, mercury intrusion, thermometry, and density measurement take into account the assumption of the capability to access the interior pores for its determination. However, this condition is very often not achieved and the characterization is only valid for the surface area.

Another crucial limitation is related to mercury intrusion, due to the methodology can damage the samples and deform the shape of the pores. This weakness makes it impossible to reuse the measured nanofibers from electrospinning after the characterization step.

2. Research Proposal: a new methodology to determine intra-fiber porosity

2.1. Objectives and hypothesis

The goal of this proposal is to develop a new characterization methodology in order to determine the intra-fiber porosity of electrospun nanofibers. A wire drum should be used in the electrospinning setup with the aim of achieving aligned fibers for the characterization step, focusing on glassy fibers. The last assumption is crucial because the cross-sectional images are more difficult to get because they could be distorted during the fiber's cutting in the case of rubbery fibers.

The proposed method includes the combination of the scanning electron microscopy (SEM) and atomic force microscopy (AFM) as means to characterize the internally porous fiber and melting fiber (without intra-fiber porosity), respectively.

2.2. The new methodology we propose

2.2.1. Electrospinning process

Fig. (7) shows a schematic representation of the electrospinning equipment that should be used. The polymer solution should be placed in a syringe that

should be connected to a single-needle. A pump system should be utilized to provide a constant solution flow through the needle. A wire drum collector should be connected to the ground wire and also it should have the same speed or higher than the polymer ejection. A high voltage power supply should be used to generate an electric field between the needle and the collector. Electrospinning experiments should be performed in a controlled chamber where the temperature and humidity are tested during the experimentation time. The dry air should be constantly renovated with an input and output flow.

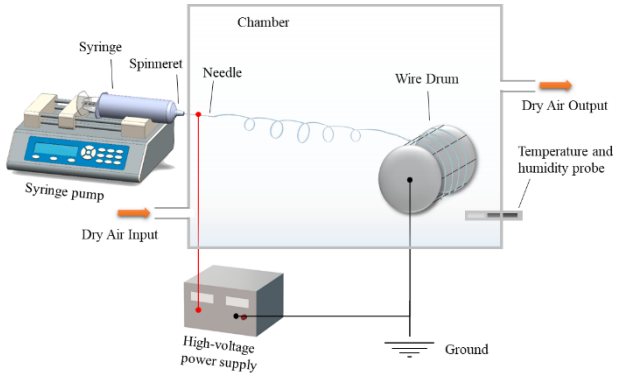

Figure 7. Electrospinning setup.

2.2.2. Sample preparation

For the samples of aligned nanofibers, a silicon wafer should be cleaned with nitrogen gas. The nanofibers should be taken from the wire drum and cut into two pieces on the previous silicon wafer.

2.2.3. Characterization of intra-fiber porosity

Throughout the research proposal section, we define the following summary statistics:

i = the number of the sample,
n = the number of the last sample,
N = the sample size.

Characterization methodology should be evaluated by scanning electron microscopy (SEM) and by atomic force microscopy (AFM). The fiber areas of the cross-section should be determined from SEM and AFM images from the same silicon wafer, which should be cut in two pieces for each image, respectively.

For analyzing the SEM images, the broken piece of unmelted nanofiber (Fig. (9) (3.a.)) should be coated by gold before. The measured diameter can be computed due to the area of porous (unmelted) electrospun fiber ($A_{unmelted}$) can be calculated taking into account the diameter of porous electrospun fiber ($D_{unmelted}$) (Fig. (9) (3.c.)):

$$A_{unmelted} = \frac{\pi \cdot D_{unmelted}^2}{4} \qquad (1)$$

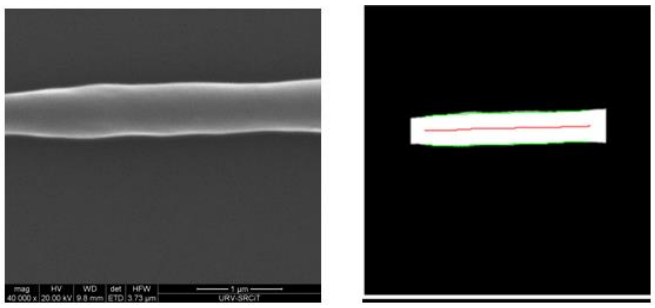

Figure 8. Example of Fiji Ridge Detection Tool.[74]

We calculate $A_{unmelted}$ for each pixel and then take the average. The single fiber SEM images used for porosity determination were post-processed using ImageJ's Ridge Detection plugin (http://fiji.sc/Ridge_Detection),[75] whereby we created a binary image of the fiber, and then a backbone ("skeleton") by the Ridge Detection plugin,[75] and the fiber width was automatically determined at different locations along the length of the fiber (Fig. FFIJI). The areas at all locations were calculated from the width taken as diameter and were then averaged (to obtain $A_{unmelted}$).

For analyzing the AFM images, the broken piece of unmelted nanofiber (Fig. (9) (4.a.)) should be melted with a temperature above the glass transition temperature (T_g). In addition, the volume of melted electrospun fiber (V_{melted}) can be determined from the AFM images (Fig. (9) (4.b.)) and considering the Eq. (2), it is possible to compute the cross-section area of melted electrospun fiber (A_{melted}) making use of the length of melted electrospun fiber (L_{melted}) (Fig. (9) (4.c.)):

$$V_{melted} = A_{melted} \cdot L_{melted} \qquad (2)$$

Considering the hypothesis that the length remains constant after the melting treatment for the AFM measurements, the porosity of the fiber (Φ_i) can be simplified as follow:

$$\Phi_i = 1 - \left(\frac{A_{melted}}{A_{unmelted}}\right) \quad (3)$$

Thus, Eq. (4) expresses their arithmetic mean of the samples, which is carried out by Profilm software and it gives a value of the intra-fiber porosity of the electrospun nanofibers ($\bar{\Phi}$).

$$\bar{\Phi} = \frac{\sum_{i=1}^{n} \Phi_i}{N} \quad (4)$$

Utilizing the Eq. (5), the sample standard deviation can be computed. Therefore, the sum of the difference between the intra-fiber porosity measurement of each sample (Φ_i) and the arithmetic mean of the total samples ($\bar{\Phi}$) gives a value which is divided by the total number of samples (N) minus one. Hence, the overall square root provides the value of the sample standard deviation for the intra-fiber porosity of the measured electrospun nanofibers.

$$\varepsilon = \sqrt{\frac{\sum_{i=1}^{n} \Phi_i - \bar{\Phi}}{N-1}} \quad (5)$$

Another consideration that should be evaluated is the crystallization of nanofibers during the melting process before the AFM, due to the temperature is above the glass transition temperature and the polymer structure can be reorganized. This procedure is necessary in order to fix the fiber to the silicon wafer and avoid the pores inside the nanofiber but can induce an error caused by a change in the density, which depends on the polymer crystallinity inasmuch as density is the mass divided by volume.

For this reason, it is crucial to use a blank test with the aim of validating our method. This blank test would be composed of compact fibers and also be tested in the melting process. Accordingly, the differential scanning calorimetry (DSC) technique would estimate the deviation of the results and the correction factor would be applied for all of them.[76]

2.3. Proof of concept data: Example data

To obtain porosity we imaged one fiber by SEM at 90º inclination and the same fiber by AFM after melting it. SEM images were obtained at 15 locations on the unmelted fiber, some of which are shown in Fig. (10) The average cross-sectional area was obtained from each of these (see Methods), and the average from these 15 areas was found to be 0.2985 μm^2 (by using Fiji Ridge Detection tool), corresponding to a 616 nm diameter fiber. For the melted sample of the same fiber, AFM images were taken at 4 different locations (Fig. 11), and their volumes were computed in Profilm Online (profilmonline.com). The average area for each was

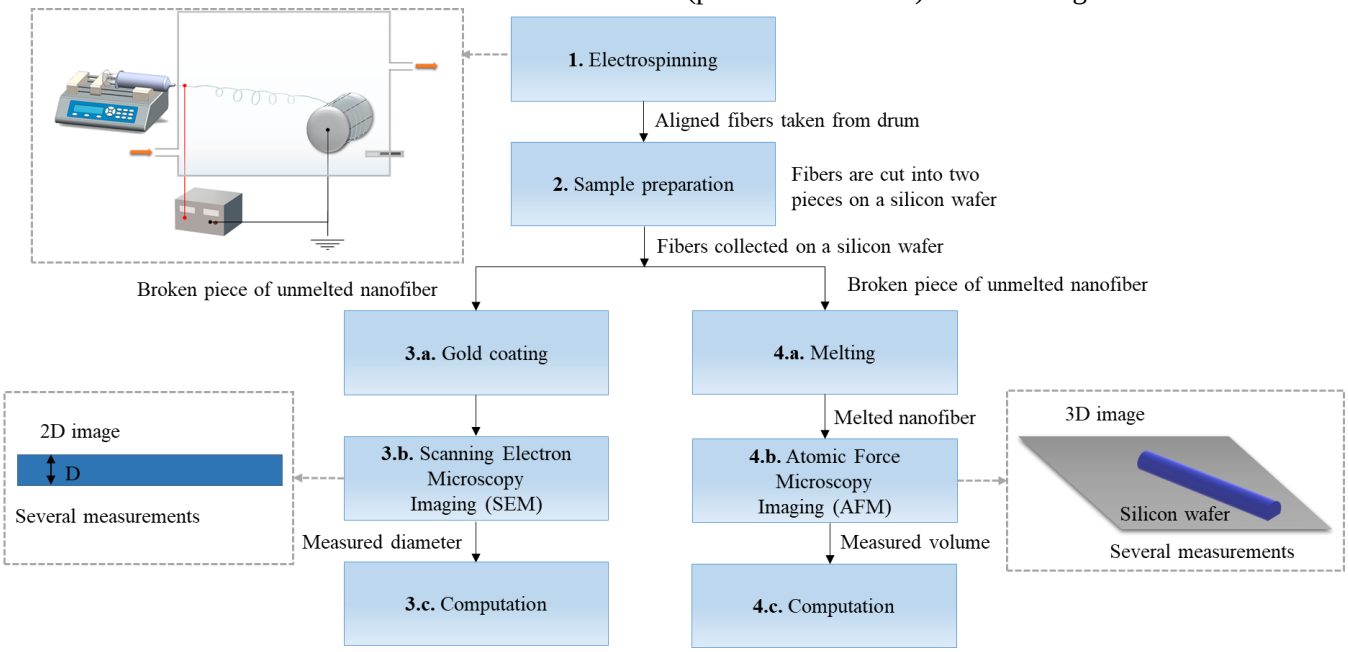

Figure 9. Schematic representation of the research proposal.

computed by dividing its volume by its length, which was computed using Gwyddion (Version 2.55). The average area for the five melted fiber sections was found to be 0.2749 μm^2. This corresponds to 7.91 % porosity; Φ=0.0791.

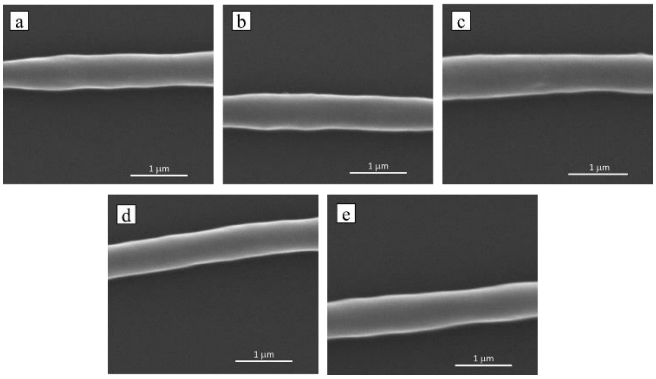

Figure 10. SEM images of internally porous polycaprolactone (PCL) nanofibers.[74]

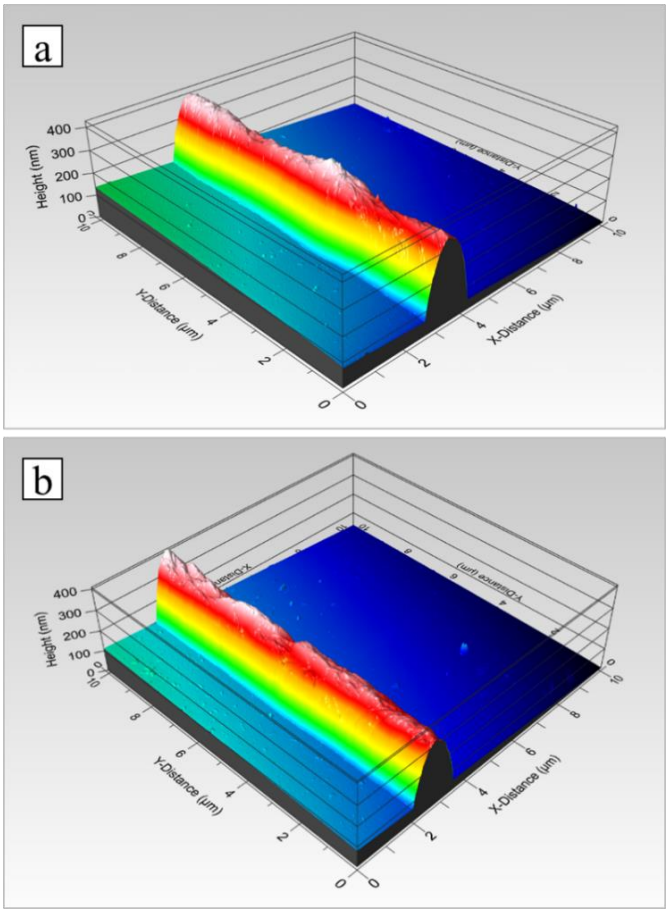

Figure 11. AFM images of melted polycaprolactone (PCL) nanofibers.[74]

2.4. Proposed research scope

The scope of the proposed research claims to analyze the characterization methodology changing different operational, solution, and ambient parameters to obtain a variety of different intra-fiber porosity that provides the reliability of the study.

The experimental work would be focused on the polystyrene (PS) and poly(methyl methacrylate) etheir intra-fiber porosity is a key factor in some applications (e. g. oil sorption[33] sensing,[43,44]). Their selection criteria of being a glassy polymer due to a rubbery polymer may cause problems of distorted cross-section images derived from SEM.

Polystyrene has been studied by numerous researches like Zheng *et al.*, which used a vapor induced phase separation (VIPS) mechanism for obtaining internally porous fibers with a smooth surface from 25% (w/v) of PS/N,N-dimethylformamide (DMF) mixture.[29] In the same way, Lu & Xia supplied evidence of the crucial role of relative humidity for the pores and wrinkles formation in the electrospinning experiments with this polymer.[26] Regarding the applications, Dong *et al.* demonstrated how internally porous PS fibers that were coated in polydopamine could evidence an enhanced capillary effect in comparison with the compact PS nanofibers. This improvement was caused by a large number of nanochannels into the fibers and it showed a new approach for the fields of sportswear, activewear, and workwear, where the thermo-physiological comfort is considered the most relevant issue.[77] All of them are examples of the possibility to generate intra-fiber porosity for its analysis.

Poly (methyl methacrylate) is a non-toxic material used in medical applications, such as tissue engineering and scaffolds.[2] In order to produce internal porosity in PMMA fibers, Li *et al.* reported the relevant role of the vapor induced phase separation (VIPS) with high relative humidity in solvent mixtures of DMF and dichloromethane (DMF).[78] Another significant approach is its triboelectric effect that provides the transformation of mechanical energy into electricity as an electrical generator.[79]

Operational parameters are pivotal with the aim of testing the internal morphology of the fibers and the limitations of the characterization method. These tested parameters would be flow rate, applied voltage, rate of a rotational collector, needle tip-to-collector distance, and

configuration of the electrodes during the electrospinning.

The introduced solution parameters for the proposed research would be the concentration of the polymer in the ejected solution during the electrospinning, viscosity, and the utilization of solvent mixtures that change the pores generation into the nanofibers.

In the electrospinning process, temperature and humidity of the chamber are ambient parameters that must be taken into account for the morphology of the produced nanofibers. Thereby, temperature and relative humidity control the thermodynamic instabilities that lead to polymer-rich and polymer-poor phases in the vapor induced phase separation phenomena (VIPS). These separation phases are required for the aim of creating uniform bead free nanofibers with an internally porous structure.[11] This homogeneous morphology of nanofibers is crucial for the reliability of the results due to the intra-fiber porosity should be measured along the fibers in order to obtain a mean value.

Another mechanism where the water of humidity, as a non-solvent, has an important role is the water imprinting by breath figure formation (BFF). Therefore, the BFF occurs when the condensed water is minimum onto the surface of the fiber and the evaporation is fast.[57] This mechanism has a tiny contribution in the calculation of the total intra-fiber porosity, however, it has to be taken into account depending on the precision of the AFM. Therefore, a high-resolution AFM characterization is capable of testing these breath figures formation (if they exist) onto the surface of nanofibers, but the AFM characterization that does not measure the breath figures can lead to mistakes in the data interpretation.

Hence, in order to minimize the random error during the proposed characterization methodology, the variability of the results should be analyzed. In this sense, a Gaussian distribution in the measurements implies the requirement of studying more samples with the aim of obtaining reliable conclusions. However, a narrow distribution of the results reduces the number of needed measurements, due to the porosity values not showing large differences upon sampling.

Moreover, the storage of the nanofibers is another parameter to study due to polymer biodegradation can be an approach for tissue engineering, but also a disadvantage for the porosity characterization because intra-fiber porosity can be distorted along the time.

3. Conclusions

In this research proposal, we review the literature about the intra-fiber porosity of electrospun nanofibers, the mechanisms to create porous electrospun nanofibers and their applications in different fields. It is useful to define intra-fiber porosity as the voids inside the nanofiber and the pores in the shell along its length.[26–28]

Intra-fiber porosity is a critical property in many applications, such as oil sorption,[8,32–34] tissue engineering,[35,36] photocatalysis,[37] drug delivery,[38] lithium-ion batteries,[40,41] sportswear,[42] and sensors.[43,44] Mechanisms to create intra-fiber porosity include heat-treated and non-heat-treated electrospun nanofibers. The former involves the porosity induced by selective removal of a sacrificial phase, emulsion electrospinning, and coaxial electrospinning with a process of calcination or pyrolysis. The latter comprises the nonsolvent induced phase separation (NSIPS), thermally induced phase separation (TIPS), vapor induced phase separation (VIPS), utilization of solvent mixtures, vitrification process, and coaxial electrospinning with an evaporation step of the core solution.

Whereas all previous works have focused on the characterization of the surface areas of electrospun fibers, we propose a simple and robust characterization method to determine intra-fiber porosity. This method could be applied to a single fiber in order to study its porous morphology. It is applicable to a wide range of polymer materials and operational, solution, and ambient conditions. The method could be perfected to determine the distribution of porosity along the length of the electrospun fiber and it could be established a correlation between the position in the nanofiber and the intra-fiber porosity in this cross-sectional area. This approach avoids the change of porosity depending on the position of the fiber that we measured.

For the purpose of increasing statistics, the proposed method requires manipulating single fibers and consequently, it is crucial to repeat several times the characterization method. Another limitation is the crystallization events during the melting process before the Atomic Force Microscopy (AFM) process. The crystallization process leads to distorted results due to the polymer structure can be reorganized and the measured cross-sectional area can give a value which is lower than the real one.

Regarding the rubbery materials, their electrospun fibers can be distorted in the cutting process for the

sample preparation. For this reason, this proposed study works better for glassy material as they break easily and the cross-section area is constant during the experimentation time.

Acknowledgments

This work was affected by the COVID-19 pandemic situation. However, I would like to acknowledge Dr. Joan Rosell-Llompart and Ph.D. student Reyda Akdemir for their advice, scientific guidance and personal recommendations during this unusual situation despite the change of way for the original Master Thesis Project.

References

(1) Xue, J.; Wu, T.; Dai, Y.; Xia, Y. Electrospinning and Electrospun Nanofibers: Methods, Materials, and Applications. *Chem. Rev.* **2019**, *119* (8), 5298–5415. https://doi.org/10.1021/acs.chemrev.8b00593.

(2) Greiner, A.; Wendorff, J. H. Electrospinning: A Fascinating Method for the Preparation of Ultrathin Fibers. *Angew. Chemie - Int. Ed.* **2007**, *46* (30), 5670–5703. https://doi.org/10.1002/anie.200604646.

(3) Xue, J.; Xie, J.; Liu, W.; Xia, Y. Electrospun Nanofibers: New Concepts, Materials, and Applications. *Acc. Chem. Res.* **2017**, *50* (8), 1976–1987. https://doi.org/10.1021/acs.accounts.7b00218.

(4) Asmatulu, R.; Khan, W. S. Chapter 2 - Historical Background of the Electrospinning Process. In *Micro and Nano Technologies*; Asmatulu, R., Khan, W. S. B. T.-S. and A. of E. N., Eds.; Elsevier, 2019; pp 17–39. https://doi.org/https://doi.org/10.1016/B978-0-12-813914-1.00002-X.

(5) Jeun, J. P.; Lim, Y. M.; Nho, Y. C. Study on Morphology of Electrospun Poly(Caprolactone) Nanofiber. *Journal of Industrial and Engineering Chemistry*. 2005, pp 573–578.

(6) Uyar, T.; Besenbacher, F. Electrospinning of Uniform Polystyrene Fibers: The Effect of Solvent Conductivity. *Polymer (Guildf).* **2008**, *49* (24), 5336–5343. https://doi.org/10.1016/j.polymer.2008.09.025.

(7) Bazilevsky, A. V; Yarin, A. L.; Megaridis, C. M. Co-Electrospinning of Core−Shell Fibers Using a Single-Nozzle Technique. *Langmuir* **2007**, *23* (5), 2311–2314. https://doi.org/10.1021/la063194q.

(8) Zaarour, B.; Zhu, L.; Huang, C.; Jin, X. Controlling the Secondary Surface Morphology of Electrospun PVDF Nanofibers by Regulating the Solvent and Relative Humidity. *Nanoscale Res. Lett.* **2018**, *13* (1), 285. https://doi.org/10.1186/s11671-018-2705-0.

(9) Kiselev, P.; Rosell-Llompart, J. Highly Aligned Electrospun Nanofibers by Elimination of the Whipping Motion. *J. Appl. Polym. Sci.* **2012**, *125* (3), 2433–2441. https://doi.org/10.1002/app.36519.

(10) Zhang, X.; Chen, J.; Zeng, Y. Construction of Helical Nanofibers from Cellulose Acetate and a Flexible Component. *Cellulose* **2019**, *26* (9), 5187–5199. https://doi.org/10.1007/s10570-019-02478-x.

(11) Fashandi, H.; Karimi, M. Characterization of Porosity of Polystyrene Fibers Electrospun at Humid Atmosphere. *Thermochim. Acta* **2012**, *547*, 38–46. https://doi.org/10.1016/j.tca.2012.08.003.

(12) Dalton, P. D.; Klee, D.; Möller, M. Electrospinning with Dual Collection Rings. *Polymer (Guildf).* **2005**, *46* (3), 611–614. https://doi.org/https://doi.org/10.1016/j.polymer.2004.11.075.

(13) Teo, W. E.; Ramakrishna, S. A Review on Electrospinning Design and Nanofibre Assemblies. *Nanotechnology* **2006**, *17* (14), R89–R106. https://doi.org/10.1088/0957-4484/17/14/r01.

(14) Katta, P.; Alessandro, M.; Ramsier, R. D.; Chase, G. G. Continuous Electrospinning of Aligned Polymer Nanofibers onto a Wire Drum Collector. *Nano Lett.* **2004**, *4* (11), 2215–2218. https://doi.org/10.1021/nl0486158.

(15) Xu, C. Y.; Inai, R.; Kotaki, M.; Ramakrishna, S. Aligned Biodegradable Nanofibrous Structure: A Potential Scaffold for Blood Vessel Engineering. *Biomaterials* **2004**, *25* (5), 877–886. https://doi.org/https://doi.org/10.1016/S0142-9612(03)00593-3.

(16) Teo, W. E.; Kotaki, M.; Mo, X. M.; Ramakrishna, S. Porous Tubular Structures with Controlled Fibre Orientation Using a Modified Electrospinning Method. *Nanotechnology* **2005**, *16* (6), 918–924. https://doi.org/10.1088/0957-4484/16/6/049.

(17) Yang, D.; Lu, B.; Zhao, Y.; Jiang, X. Fabrication of Aligned Fibrous Arrays by Magnetic Electrospinning. *Adv. Mater.* **2007**, *19* (21), 3702–3706. https://doi.org/10.1002/adma.200700171.

(18) Liu, Y.; Zhang, X.; Xia, Y.; Yang, H. Magnetic-Field-Assisted Electrospinning of Aligned Straight and Wavy Polymeric Nanofibers. *Adv. Mater.* **2010**, *22* (22), 2454–2457. https://doi.org/10.1002/adma.200903870.

(19) Thoppey, N. M.; Bochinski, J. R.; Clarke, L. I.; Gorga, R. E. Unconfined Fluid Electrospun into High Quality Nanofibers from a Plate Edge. *Polymer (Guildf).* **2010**, *51* (21), 4928–4936. https://doi.org/https://doi.org/10.1016/j.polymer.2010.07.046.

(20) Lu, P.; Murray, S.; Zhu, M. Chapter 23 - Electrospun Nanofibers for Catalysts. In *Micro and Nano Technologies*; Ding, B., Wang, X., Yu, J. B. T.-E. N. and A., Eds.; William Andrew Publishing, 2019; pp 695–717. https://doi.org/https://doi.org/10.1016/B978-0-323-51270-1.00023-6.

(21) Sankar, S.; Sharma, C. S.; Rath, S. N.; Ramakrishna, S. Electrospun Nanofibres to Mimic Natural Hierarchical Structure of Tissues: Application in Musculoskeletal Regeneration. *J. Tissue Eng. Regen.*

Med. **2018**, *12* (1), e604–e619. https://doi.org/10.1002/term.2335.

(22) Shaikh, J. S.; Shaikh, N. S.; Mali, S. S.; Patil, J. V; Pawar, K. K.; Kanjanaboos, P.; Hong, C. K.; Kim, J. H.; Patil, P. S. Nanoarchitectures in Dye-Sensitized Solar Cells: Metal Oxides, Oxide Perovskites and Carbon-Based Materials. *Nanoscale* **2018**, *10* (11), 4987–5034. https://doi.org/10.1039/C7NR08350E.

(23) Zhu, M.; Han, J.; Wang, F.; Shao, W.; Xiong, R.; Zhang, Q.; Pan, H.; Yang, Y.; Samal, S. K.; Zhang, F.; et al. Electrospun Nanofibers Membranes for Effective Air Filtration. *Macromol. Mater. Eng.* **2017**, *302* (1), 1600353. https://doi.org/10.1002/mame.201600353.

(24) Medeiros, E. S.; Glenn, G. M.; Klamczynski, A. P.; Orts, W. J.; Mattoso, L. H. C. Solution Blow Spinning: A New Method to Produce Micro- and Nanofibers from Polymer Solutions. *J. Appl. Polym. Sci.* **2009**, *113* (4), 2322–2330. https://doi.org/10.1002/app.30275.

(25) Huang, C.; Thomas, N. L. Fabrication of Porous Fibers via Electrospinning: Strategies and Applications. *Polym. Rev.* **2019**, 1–53. https://doi.org/10.1080/15583724.2019.1688830.

(26) Lu, P.; Xia, Y. Maneuvering the Internal Porosity and Surface Morphology of Electrospun Polystyrene Yarns by Controlling the Solvent and Relative Humidity. *Langmuir* **2013**, *29* (23), 7070–7078. https://doi.org/10.1021/la400747y.

(27) Chen, S.; Li, R.; Li, X.; Xie, J. Electrospinning: An Enabling Nanotechnology Platform for Drug Delivery and Regenerative Medicine. *Adv. Drug Deliv. Rev.* **2018**, *132*, 188–213. https://doi.org/10.1016/j.addr.2018.05.001.

(28) Kuang, G.; Zhang, Z.; Liu, S.; Zhou, D.; Lu, X.; Jing, X.; Huang, Y. Biphasic Drug Release from Electrospun Polyblend Nanofibers for Optimized Local Cancer Treatment. *Biomater. Sci.* **2018**, *6* (2), 324–331. https://doi.org/10.1039/c7bm01018d.

(29) Zheng, J.; Zhang, H.; Zhao, Z.; Han, C. C. Construction of Hierarchical Structures by Electrospinning or Electrospraying. *Polymer (Guildf).* **2012**, *53* (2), 546–554. https://doi.org/https://doi.org/10.1016/j.polymer.2011.12.018.

(30) Lee, C. G.; Javed, H.; Zhang, D.; Kim, J. H.; Westerhoff, P.; Li, Q.; Alvarez, P. J. J. Porous Electrospun Fibers Embedding TiO2 for Adsorption and Photocatalytic Degradation of Water Pollutants. *Environ. Sci. Technol.* **2018**, *52* (7), 4285–4293. https://doi.org/10.1021/acs.est.7b06508.

(31) Dai, Y.; Niu, J.; Liu, J.; Yin, L.; Xu, J. In Situ Encapsulation of Laccase in Microfibers by Emulsion Electrospinning: Preparation, Characterization, and Application. *Bioresour. Technol.* **2010**, *101* (23), 8942–8947. https://doi.org/10.1016/j.biortech.2010.07.027.

(32) Bandegi, A.; Moghbeli, M. R. Effect of Solvent Quality and Humidity on the Porous Formation and Oil Absorbency of SAN Electrospun Nanofibers. *J. Appl. Polym. Sci.* **2018**, *135* (1), 1–13. https://doi.org/10.1002/app.45586.

(33) Isık, T.; Demir, M. M. Tailored Electrospun Fibers from Waste Polystyrene for High Oil Adsorption. *Sustain. Mater. Technol.* **2018**, *18*, e00084. https://doi.org/https://doi.org/10.1016/j.susmat.2018.e00084.

(34) Chen, P.-Y.; Tung, S.-H. One-Step Electrospinning To Produce Nonsolvent-Induced Macroporous Fibers with Ultrahigh Oil Adsorption Capability. *Macromolecules* **2017**, *50* (6), 2528–2534. https://doi.org/10.1021/acs.macromol.6b02696.

(35) Mota, C.; Wang, S.-Y.; Puppi, D.; Gazzarri, M.; Migone, C.; Chiellini, F.; Chen, G.-Q.; Chiellini, E. Additive Manufacturing of Poly[(R)-3-Hydroxybutyrate-Co-(R)-3-Hydroxyhexanoate] Scaffolds for Engineered Bone Development. *J. Tissue Eng. Regen. Med.* **2017**, *11* (1), 175–186. https://doi.org/10.1002/term.1897.

(36) Puppi, D.; Mota, C.; Gazzarri, M.; Dinucci, D.; Gloria, A.; Myrzabekova, M.; Ambrosio, L.; Chiellini, F. Additive Manufacturing of Wet-Spun Polymeric Scaffolds for Bone Tissue Engineering. *Biomed. Microdevices* **2012**, *14* (6), 1115–1127. https://doi.org/10.1007/s10544-012-9677-0.

(37) Hou, H.; Wang, L.; Gao, F.; Wei, G.; Zheng, J.; Tang, B.; Yang, W. Hierarchically Porous TiO2/SiO2 Fibers with Enhanced Photocatalytic Activity. *RSC Adv.* **2014**, *4* (38), 19939–19944. https://doi.org/10.1039/C4RA02285H.

(38) Honarbakhsh, S.; Pourdeyhimi, B. Scaffolds for Drug Delivery, Part I: Electrospun Porous Poly(Lactic Acid) and Poly(Lactic Acid)/Poly(Ethylene Oxide) Hybrid Scaffolds. *J. Mater. Sci.* **2011**, *46* (9), 2874–2881. https://doi.org/10.1007/s10853-010-5161-5.

(39) Brown, T. D.; Dalton, P. D.; Hutmacher, D. W. Melt Electrospinning Today: An Opportune Time for an Emerging Polymer Process. *Prog. Polym. Sci.* **2016**, *56*, 116–166. https://doi.org/https://doi.org/10.1016/j.progpolymsci.2016.01.001.

(40) Sabetzadeh, N.; Gharehaghaji, A. A.; Javanbakht, M. Porous PAN Micro/Nanofiber Separators for Enhanced Lithium-Ion Battery Performance. *Solid State Ionics* **2018**, *325*, 251–257. https://doi.org/https://doi.org/10.1016/j.ssi.2018.08.013.

(41) Yu, Y.; Xiong, S.; Huang, H.; Zhao, L.; Nie, K.; Chen, S.; Xu, J.; Yin, X.; Wang, H.; Wang, L. Fabrication and Application of Poly (Phenylene Sulfide) Ultrafine Fiber. *React. Funct. Polym.* **2020**, *150*, 104539. https://doi.org/https://doi.org/10.1016/j.reactfunctpolym.2020.104539.

(42) Yan, W.; Miao, D.; Babar, A. A.; Zhao, J.; Jia, Y.; Ding, B.; Wang, X. Multi-Scaled Interconnected Inter- and Intra-Fiber Porous Janus Membranes for

Enhanced Directional Moisture Transport. *J. Colloid Interface Sci.* **2020**, *565*, 426–435. https://doi.org/https://doi.org/10.1016/j.jcis.2020.01.063.

(43) Kim, W.; Park, E.; Jeon, S. Performance Enhancement of a Quartz Tuning Fork Sensor Using a Cellulose Nanocrystal-Reinforced Nanoporous Polymer Fiber. *Sensors* **2020**, *20* (2). https://doi.org/10.3390/s20020437.

(44) Nathani, A.; Sharma, C. S. Electrospun Mesoporous Poly(Styrene-Block-Methyl- Methacrylate) Nanofibers as Biosensing Platform: Effect of Fibers Porosity on Sensitivity. *Electroanalysis* **2019**, *31* (11), 2138–2144. https://doi.org/10.1002/elan.201800796.

(45) Gupta, A.; Saquing, C. D.; Afshari, M.; Tonelli, A. E.; Khan, S. A.; Kotek, R. Porous Nylon-6 Fibers via a Novel Salt-Induced Electrospinning Method. *Macromolecules* **2009**, *42* (3), 709–715. https://doi.org/10.1021/ma801918c.

(46) Peng, M.; Li, D.; Shen, L.; Chen, Y.; Zheng, Q.; Wang, H. Nanoporous Structured Submicrometer Carbon Fibers Prepared via Solution Electrospinning of Polymer Blends. *Langmuir* **2006**, *22* (22), 9368–9374. https://doi.org/10.1021/la061154g.

(47) Zhang, L.; Hsieh, Y. Lo. Nanoporous Ultrahigh Specific Surface Polyacrylonitrile Fibres. *Nanotechnology* **2006**, *17* (17), 4416–4423. https://doi.org/10.1088/0957-4484/17/17/022.

(48) Zhang, Z.; Li, X.; Wang, C.; Fu, S.; Liu, Y.; Shao, C. Polyacrylonitrile and Carbon Nanofibers with Controllable Nanoporous Structures by Electrospinning. *Macromol. Mater. Eng.* **2009**, *294* (10), 673–678. https://doi.org/10.1002/mame.200900076.

(49) Yusof, N.; Ismail, A. F. Post Spinning and Pyrolysis Processes of Polyacrylonitrile (PAN)-Based Carbon Fiber and Activated Carbon Fiber: A Review. *J. Anal. Appl. Pyrolysis* **2012**, *93*, 1–13. https://doi.org/https://doi.org/10.1016/j.jaap.2011.10.001.

(50) Guo, J.; Shu, J.; Nie, J.; Ma, G. Fe/Ni Bimetal and Nitrogen Co-Doped Porous Carbon Fibers as Electrocatalysts for Oxygen Reduction Reaction. *J. Colloid Interface Sci.* **2020**, *560*, 330–337. https://doi.org/https://doi.org/10.1016/j.jcis.2019.09.101.

(51) Li, D.; Xia, Y. Fabrication of Titania Nanofibers by Electrospinning. *Nano Lett.* **2003**, *3* (4), 555–560. https://doi.org/10.1021/nl034039o.

(52) Adhikari, S. P.; Pant, H. R.; Mousa, H. M.; Lee, J.; Kim, H. J.; Park, C. H.; Kim, C. S. Synthesis of High Porous Electrospun Hollow TiO2 Nanofibers for Bone Tissue Engineering Application. *J. Ind. Eng. Chem.* **2016**, *35*, 75–82. https://doi.org/https://doi.org/10.1016/j.jiec.2015.12.004.

(53) Cho, Y.-S.; Roh, S. H. Sol–Gel Synthesis of Porous Titania Fibers by Electro-Spinning for Water Purification. *J. Dispers. Sci. Technol.* **2018**, *39* (1), 33–44. https://doi.org/10.1080/01932691.2017.1292461.

(54) Lin, Y. P.; Chen, Y. Y.; Lee, Y. C.; Chen-Yang, Y. W. Effect of Wormhole-like Mesoporous Anatase TiO2 Nanofiber Prepared by Electrospinning with Ionic Liquid on Dye-Sensitized Solar Cells. *J. Phys. Chem. C* **2012**, *116* (24), 13003–13012. https://doi.org/10.1021/jp212146p.

(55) Chen, H.; Di, J.; Wang, N.; Dong, H.; Wu, J.; Zhao, Y.; Yu, J.; Jiang, L. Fabrication of Hierarchically Porous Inorganic Nanofibers by a General Microemulsion Electrospinning Approach. *Small* **2011**, *7* (13), 1779–1783. https://doi.org/10.1002/smll.201002376.

(56) Singh, N.; Salam, Z.; Subasri, A.; Sivasankar, N.; Subramania, A. Development of Porous TiO2 Nanofibers by Solvosonication Process for High Performance Quantum Dot Sensitized Solar Cell. *Sol. Energy Mater. Sol. Cells* **2018**, *179*, 417–426. https://doi.org/https://doi.org/10.1016/j.solmat.2018.01.042.

(57) Bodnár, E.; Grifoll, J.; Rosell-Llompart, J. Polymer Solution Electrospraying: A Tool for Engineering Particles and Films with Controlled Morphology. *J. Aerosol Sci.* **2018**, *125* (May), 93–118. https://doi.org/10.1016/j.jaerosci.2018.04.012.

(58) Huang, C.; Thomas, N. L. Fabricating Porous Poly(Lactic Acid) Fibres via Electrospinning. *Eur. Polym. J.* **2018**, *99* (September 2017), 464–476. https://doi.org/10.1016/j.eurpolymj.2017.12.025.

(59) Pai, C. L.; Boyce, M. C.; Rutledge, G. C. Morphology of Porous and Wrinkled Fibers of Polystyrene Electrospun from Dimethylformamide. *Macromolecules* **2009**, *42* (6), 2102–2114. https://doi.org/10.1021/ma802529h.

(60) Semiromi, F. B.; Nejaei, A.; Shojaee, M. Effect of Methanol Concentration on the Morphology and Wettability of Electrospun Nanofibrous Membranes Based on Polycaprolactone for Oil-Water Separation. *Fibers Polym.* **2019**, *20* (12), 2453–2460. https://doi.org/10.1007/s12221-019-1047-6.

(61) Fashandi, H.; Ghomi, A. Interplay of Phase Separation and Physical Gelation in Morphology Evolution within Nanoporous Fibers Electrospun at High Humidity Atmosphere. *Ind. Eng. Chem. Res.* **2015**, *54* (1), 240–253. https://doi.org/10.1021/ie503848v.

(62) Dror, Y.; Salalha, W.; Avrahami, R.; Zussman, E.; Yarin, A. L.; Dersch, R.; Greiner, A.; Wendorff, J. H. One-Step Production of Polymeric Microtubes by Co-Electrospinning. *Small* **2007**, *3* (6), 1064–1073. https://doi.org/10.1002/smll.200600536.

(63) Zhao, Y.; Cao, X.; Jiang, L. Bio-Mimic Multichannel Microtubes by a Facile Method. *J. Am. Chem. Soc.* **2007**, *129* (4), 764–765. https://doi.org/10.1021/ja068165g.

(64) Zhang, J.; Mensah, A.; Narh, C.; Hou, X.; Cai, Y.;

Qiao, H.; Wei, Q. Fabrication of Flexible TiO2-SiO2 Composite Nanofibers with Variable Structure as Efficient Adsorbent. *Ceram. Int.* **2020**, *46* (3), 3543–3549. https://doi.org/https://doi.org/10.1016/j.ceramint.2019.10.071.

(65) Rouquerol, J.; Avnir, D.; Fairbridge, C. W.; Everett, D. H.; Haynes, J. M.; Pernicone, N.; Ramsay, J. D. F.; Sing, K. S. W.; Unger, K. K. Recommendations for the Characterization of Porous Solids (Technical Report). *Pure Appl. Chem.* **1994**, *66* (8), 1739–1758. https://doi.org/https://doi.org/10.1351/pac199466081739.

(66) Léon Y León, C. A. New Perspectives in Mercury Porosimetry. *Adv. Colloid Interface Sci.* **1998**, *76–77*, 341–372. https://doi.org/10.1016/S0001-8686(98)00052-9.

(67) Landry, M. R. Thermoporometry by Differential Scanning Calorimetry: Experimental Considerations and Applications. *Thermochim. Acta* **2005**, *433* (1), 27–50. https://doi.org/https://doi.org/10.1016/j.tca.2005.02.015.

(68) Campo, E. M.; Yates, D.; Berson, B.; Rojas, W.; Winter, A. D.; Ananth, M.; Santiago-Aviles, J. J.; Terentjev, E. M. Tomography of Electrospun Carbon Nanotube Polymeric Blends by Focus Ion Beam: Alignment and Phase Separation Analysis from Multicontrast Electron Imaging. *Macromol. Mater. Eng.* **2017**, *302* (8), 1600479. https://doi.org/10.1002/mame.201600479.

(69) Stachewicz, U.; Szewczyk, P. K.; Kruk, A.; Barber, A. H.; Czyrska-Filemonowicz, A. Pore Shape and Size Dependence on Cell Growth into Electrospun Fiber Scaffolds for Tissue Engineering: 2D and 3D Analyses Using SEM and FIB-SEM Tomography. *Mater. Sci. Eng. C* **2019**, *95*, 397–408. https://doi.org/https://doi.org/10.1016/j.msec.2017.08.076.

(70) Stachewicz, U.; Qiao, T.; Rawlinson, S. C. F.; Almeida, F. V.; Li, W.-Q.; Cattell, M.; Barber, A. H. 3D Imaging of Cell Interactions with Electrospun PLGA Nanofiber Membranes for Bone Regeneration. *Acta Biomater.* **2015**, *27*, 88–100. https://doi.org/https://doi.org/10.1016/j.actbio.2015.09.003.

(71) Szewczyk, P. K.; Metwally, S.; Karbowniczek, J. E.; Marzec, M. M.; Stodolak-Zych, E.; Gruszczyński, A.; Bernasik, A.; Stachewicz, U. Surface-Potential-Controlled Cell Proliferation and Collagen Mineralization on Electrospun Polyvinylidene Fluoride (PVDF) Fiber Scaffolds for Bone Regeneration. *ACS Biomater. Sci. Eng.* **2019**, *5* (2), 582–593. https://doi.org/10.1021/acsbiomaterials.8b01108.

(72) Liu, W.; Huang, C.; Jin, X. Electrospinning of Grooved Polystyrene Fibers: Effect of Solvent Systems. *Nanoscale Res. Lett.* **2015**, *10* (1), 237. https://doi.org/10.1186/s11671-015-0949-5.

(73) Abd Mutalib, M.; Rahman, M. A.; Othman, M. H. D.; Ismail, A. F.; Jaafar, J. Chapter 9 - Scanning Electron Microscopy (SEM) and Energy-Dispersive X-Ray (EDX) Spectroscopy; Hilal, N., Ismail, A. F., Matsuura, T., Oatley-Radcliffe, D. B. T.-M. C., Eds.; Elsevier, 2017; pp 161–179. https://doi.org/https://doi.org/10.1016/B978-0-444-63776-5.00009-7.

(74) Akdemir, R. Personal Communication. **2020**.

(75) Steger, C. An Unbiased Detector of Curvilinear Structures. *IEEE Trans. Pattern Anal. Mach. Intell.* **1998**, *20* (2), 113–125. https://doi.org/10.1109/34.659930.

(76) Kong, Y.; Hay, J. N. The Measurement of the Crystallinity of Polymers by DSC. *Polymer (Guildf).* **2002**, *43* (14), 3873–3878. https://doi.org/https://doi.org/10.1016/S0032-3861(02)00235-5.

(77) Dong, Y.; Kong, J.; Phua, S. L.; Zhao, C.; Thomas, N. L.; Lu, X. Tailoring Surface Hydrophilicity of Porous Electrospun Nanofibers to Enhance Capillary and Push–Pull Effects for Moisture Wicking. *ACS Appl. Mater. Interfaces* **2014**, *6* (16), 14087–14095. https://doi.org/10.1021/am503417w.

(78) Li, L.; Jiang, Z.; Li, M.; Li, R.; Fang, T. Hierarchically Structured PMMA Fibers Fabricated by Electrospinning. *RSC Adv.* **2014**, *4* (95), 52973–52985. https://doi.org/10.1039/c4ra05385k.

(79) Busolo, T.; Ura, D. P.; Kim, S. K.; Marzec, M. M.; Bernasik, A.; Stachewicz, U.; Kar-Narayan, S. Surface Potential Tailoring of PMMA Fibers by Electrospinning for Enhanced Triboelectric Performance. *Nano Energy* **2019**, *57*, 500–506. https://doi.org/https://doi.org/10.1016/j.nanoen.2018.12.037.